Subducted and Melanotic Cells in Advanced Age-Related Macular Degeneration Are Derived From Retinal Pigment Epithelium

Emma C. Zanzottera,[1,2] Jeffrey D. Messinger,[1] Thomas Ach,[1,3] R. Theodore Smith,[4] and Christine A. Curcio[1]

[1]Department of Ophthalmology, University of Alabama School of Medicine, Birmingham, Alabama, United States
[2]Eye Clinic, Department of Clinical Science "Luigi Sacco," Sacco Hospital, University of Milan, Milan, Italy
[3]University Hospital of Würzburg, Department of Ophthalmology, Würzburg, Germany
[4]Department of Ophthalmology, New York University, New York, New York, United States

Correspondence: Christine A. Curcio, Department of Ophthalmology, EyeSight Foundation of Alabama Vision Research Laboratories, 1670 University Boulevard, Room 360, University of Alabama School of Medicine, Birmingham, AL 35294-0099, USA; curcio@uab.edu.

Submitted: January 11, 2015
Accepted: April 5, 2015

Citation: Zanzottera EC, Messinger JD, Ach T, Smith RT, Curcio CA. Subducted and Melanotic cells in advanced age-related macular degeneration are derived from retinal pigment epithelium. *Invest Ophthalmol Vis Sci*. 2015;56:3269–3278. DOI:10.1167/iovs.15-16432

Purpose. To describe, illustrate, and account for two cell types plausibly derived from RPE in geographic atrophy (GA) and choroidal neovascularization (CNV) of AMD, using melanosomes, lipofuscin, and basal laminar deposit (BLamD) as anatomical markers.

Methods. Human donor eyes with GA (n = 13) or CNV (n = 39) were histologically processed, photodocumented, and analyzed for frequencies of occurrence. We defined RPE as cells containing spindle-shaped melanosomes and RPE lipofuscin, internal to basal lamina or BLamD, if present, or Bruch's membrane if not, and RPE-derived cells as those plausibly derived from RPE and not attached to basal lamina or BLamD.

Results. 'Subducted' cells contain RPE melanosomes and localize to the sub-RPE space, on Bruch's membrane. Credible transitional forms from RPE cells were seen. Grades of RPE overlying 'Subducted' cells were 'Atrophic with BLamD' (32.2% vs. 37.0% of 'Subducted,' for GA and CNV eyes, respectively), 'Dissociated' (22.0% vs. 21.7%), 'Nonuniform' (22.0% vs. 23.9%), and 'Sloughed' RPE (10.2% vs. 4.3%). Found exclusively in CNV scars, 'Melanotic' cells containing spherical melanosomes were adjacent to 'Entombed' RPE with spindle-shaped and spherical melanosomes. Of subretinal 'Melanotic' cells, 40.0% associated with 'Atrophy with BLamD,' 36.8% with 'Atrophy without BLamD,' and 20.6% with 'Entombed.'

Conclusions. 'Dissociated' RPE within atrophic areas may be the source of 'Subducted' cells. 'Entombed' RPE within fibrovascular and fibrocellular scars may be the source of 'Melanotic' cells. An imaging correlate for 'Subducted' cells awaits discovery; 'Melanotic' cells appear gray-black in the CNV fundus. Results provide a basis for future molecular phenotyping studies.

Keywords: age-related macular degeneration, retinal pigment epithelium, melanosomes, lipofuscin, histology, apoptosis, migration, transdifferentiation, basal laminar deposits

Age-related macular degeneration (AMD), a prevalent disease of the photoreceptor support system,[1] exhibits prominent pathology in the RPE and underlying Bruch's membrane (BrM). The RPE is a monolayer of cuboidal epithelial cells of neuroectodermal origin, dually tasked with maintaining retina apically and choroid basally.[2–4] As stated,[5] we hypothesize that the RPE exhibits stereotypic stress responses and death pathways, which if defined, quantified, and followed, provide windows into molecular pathology and points of therapeutic entry. We seek to systematize morphologies of RPE and RPE-derived cells in advanced AMD. The first of two companion reports focused on RPE cells, which contain melanosomes, lipofuscin, and melanolipofuscin and are associated with a basement membrane or with basal laminar deposits (BLamD).[5] Our major findings were the numerous RPE cells surviving at end-stage disease, specifically 'Dissociated' (a broken up RPE layer within the atrophic area) and 'Entombed' (cells within fibrovascular and fibrocellular scars). We also solidified and extended our previous studies[6,7] that proposed two major pathways of cell transdifferentiation and death, represented by the 'Sloughed'/'Intraretinal' and 'Shedding' morphologies, respectively.

In this second of two companion reports, we describe, illustrate, and quantify RPE-derived cells, which are plausibly derived from RPE, yet are outside the RPE layer and not attached to a basal lamina or BLamD. Transdifferentiation is the direct transformation of one differentiated cell type to another.[8] An example of transdifferentiation is the epithelium-to-mesenchymal transition (EMT), essential to embryology, in which polarized epithelial cells convert into motile mesenchymal cells, activated by contextual microenvironmental signals and governed by a network of transcription factors, epigenetic regulators, and signaling pathways.[9] Central to cancer, wound healing, and organ fibrosis, transdifferentiation by EMT may also contribute to RPE behavior in proliferative vitreoretinopathy and advanced AMD.[10–12] In this article, we focus on two types of RPE-derived cells: 'Subducted' and 'Melanotic.' We provide evidence that these distinctive morphologies arise

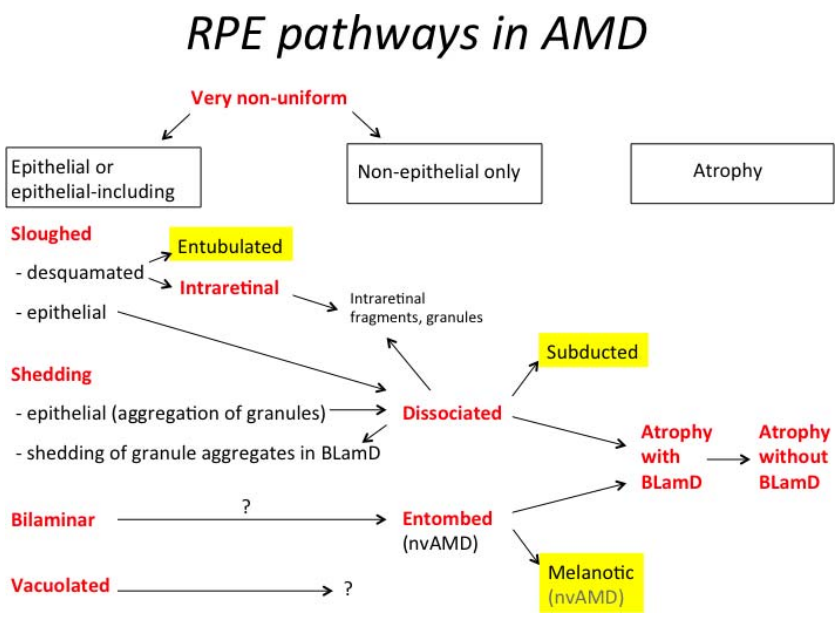

Figure 1. Graphical hypothesis of RPE pathways in AMD. This schema was initiated in our companion paper[5] and highlights in *yellow* RPE-derived cells, of which 'Subducted' and 'Melanotic' are described in this article. For reasons given in the text, the most likely sources of 'Subducted' cells are 'Dissociated' cells in the atrophic area. The most likely source of 'Melanotic' cells is 'Entombed' cells within scars. One other RPE-derived morphology is 'Entubulated,' found in the lumen of outer retinal tubulation and presented separately.[19] The most likely sources of 'Entubulated' cells are the desquamated cells of the 'Sloughed' morphology; Figure 3A shows a rare example of 'Dissociated' cells apparently entering a tubulation. The fates of RPE-derived cells are unknown and could include death, further transdifferentiation to unrecognizable forms, or emigration. For simplicity, normal aging changes are omitted from the schema, which begins with 'Very Nonuniform.' nvAMD, neovascular AMD.

directly from the 'Dissociated' and 'Entombed' RPE phenotypes, respectively, as defined in our companion article,[5] reinforcing that RPE transdifferentiation may be important in AMD pathogenesis.[10–12]

Methods

This study was performed in parallel with a companion study.[5] In brief, eyes with advanced AMD were obtained at a median death-to-preservation time 3:49 hours (range, 0:40–11:40 hours), preserved, photographed ex vivo, and prepared for submicrometer-thick macula-wide sections. A full-thickness eye wall punch 8 mm in diameter was postfixed for neutral lipid preservation, embedded in epoxy resin, sectioned at 0.8-μm thickness, and stained with toluidine blue. An initial diagnosis of AMD was made by ex vivo color fundus photography and verified histologically. To permit unbiased estimates of each morphology's frequency, we annotated sections of individual eyes from the Project MACULA website of AMD histopathology (available in the public domain at http://projectmacula.cis.uab.edu) using a systematic sampling scheme of predefined locations within each of two standard horizontal planes. A central section captured the foveal center and a section at 2 mm superior was the longest possible near the ring of high rod density (3–5 mm superior to the foveal center).[13] The nominal sampling scheme contained 25 locations in the central section and 13 in the superior section, from 3500 μm nasal to 3500 μm temporal to the fovea. Sections were photodocumented with a ×60 oil-immersion objective (numerical aperture = 1.4) and digital camera (XC10; Olympus, Center Valley, PA, USA) and viewed on a monitor at ×1900 final magnification.

Retinal pigment epithelial melanosomes are unique in the body due to their spindle shape.[14,15] They localize to the apical part of the cells and spread basally in aging.[16,17] Lipofuscin and melanolipofuscin granules are recognizable by their size (~1 μm), shape (irregular, potato-like), abundance within adult RPE, and coloration by toluidine blue stain (blue-green, tending toward bronze or brown depending on the eye). With guidance from electron microscopy images, it was possible to discriminate RPE melanosomes from the combined population of lipofuscin and melanolipofuscin granules (termed LF/MLF), which were not routinely discriminated from each other by light microscopy at these viewing magnifications.

In the companion report,[5] we described and quantified RPE cells, defined as cells containing RPE melanosomes and RPE lipofuscin, internal to basal lamina or BLamD, if present, or BrM if not.[18] We further defined the RPE layer as the plane of RPE cells located between the subretinal and sub-RPE spaces, which are divided by the RPE if present and BLamD if not. The sub-RPE space is defined as a potential space between RPE basal lamina or BLamD and the inner collagenous layer of BrM.

In this report, we describe and quantify RPE-derived cells, defined as those plausibly derived from RPE, outside the RPE layer and not attached to the basal lamina or BLamD. We particularly sought evidence of transitional forms between RPE and RPE-derived cells in intact histological sections. Frequency of occurrence for RPE-derived cells was referenced to both the total number of sampling locations and the number of locations with RPE-derived cells.[5]

Results

Figure 1 is a road map of RPE cell phenotypes defined in our companion article[5] to contextualize the RPE-derived cell phenotypes described in Table 1. Of these, we focus on 'Subducted' and 'Melanotic.' A description of 'Entubulated' was published.[19] In 13 eyes of 12 donors with geographic atrophy (GA) (8 females, 4 males, mean age 85.6 ± 4.9 years), 449 locations (150 superior and 299 central) were examined. In 39 eyes with choroidal neovascularization (CNV; 25 female, 14 males, mean age 85.4 ± 7.2 years), 1363 locations (452

Investigative Ophthalmology & Visual Science

Table 1. Definitions of RPE-Derived Cells; Frequencies in GA and CNV Eyes

Morphology*	Description	GA (Superior + Central) Frequency No. (%) of 449 Total; Range No. (%) per Eye	CNV (Superior + Central) Frequency No. (%) of 1363 Total; Range No. (%) per Eye
'Subducted'	Rounded or flattened cells, singly or in groups, in sub-RPE space.	59 (13.1%); 0–10 (0%–26.3%)	65 (4.8%); 0–12 (0%–31.6%)
'Melanotic'	Individual cells or cells in multiple layers with large black, polydisperse spherical melanosomes; associated with fibrovascular and fibrocellular scars, in subretinal or sub-RPE space.	Not present	In subretinal space: 155 (11.4%); 0–23 (0%–60.5%) In sub-RPE space: 18 (1.3%); 0–3 (0%–7.9%)
'Entubulated'	In lumen of outer retinal tubulation[19]	ND	ND

ND, not determined herein; described elsewhere.[19]
* As defined in a companion article,[5] these cells are nonepithelial (i.e., not adjacent to RPE basal lamina or BLamD).

superior and 911 central) were examined. Links to digital sections from which figures were chosen are in the Appendix.

In GA and CNV eyes, we observed pigmented cells containing spindle-shaped melanosomes and LF/MLF granules in sub-RPE space, external to BLamD and adjacent to BrM (Figs. 2, 3). These cells were very similar in granule content to nearby RPE cells and we called them 'Subducted,' adapting a geological term to convey the notion of one layer passing beneath another. 'Subducted' cells ranged in shape, from a dome with a base on BrM to ovoid to flat, with the transverse width greater than axial height for the flatter cells. Apical processes were not detectable. 'Subducted' cells could be solitary (Fig. 2C), or arranged in clusters horizontally (Figs. 2A, 2B) or vertically (Fig. 2D) and were not accompanied by pigmented cellular fragments like those near 'Shedding' or 'Dissociated' RPE.[5] Instead, they were surrounded by basal linear deposit, cellular processes (Müller cell and microglia) passing from neurosensory retina under BLamD,[20] scar (in CNV eyes only), or rarely, fluid (in CNV eyes only).[21]

The 'Subducted' designation is strengthened by compelling examples of transitional forms between granule-rich RPE atop BLamD, equally granule-rich cells within the sub-RPE space, and granule-poor cells in the same location, all within single intact histological sections. Figure 3 shows examples from

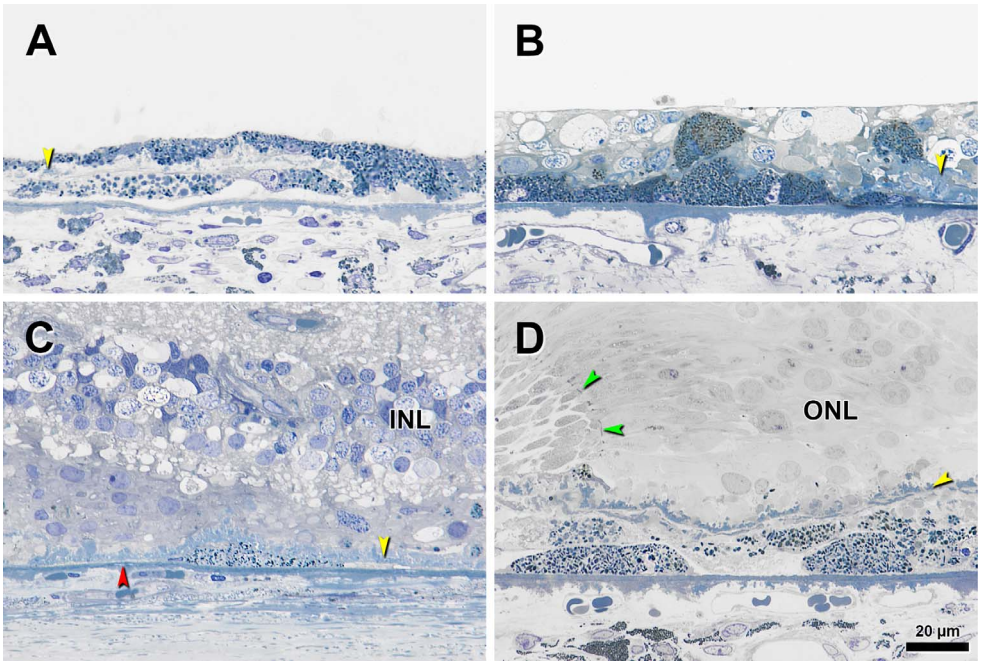

Figure 2. Subducted cells in eyes with advanced AMD. Submicrometer epoxy resin sections were stained with toluidine blue. *Yellow arrowheads*, BLamD; *red arrowhead*, calcification in BrM; *black arrowheads*, 'Subducted' cell. (**A**) Two flat cells with distinct melanin and LF/MLF granules in sub-RPE space. 'Nonuniform' RPE above a thin layer of early BLamD, parafovea. Retina is detached. (**B**) Cluster of 'Subducted' cells lying on BrM containing packed melanosomes and LF/MLF granules in an extremely thin fovea. Granular content of RPE cells inside inner nuclear layer (INL) and internal to BLamD looks similar in density and staining to the 'Subducted' cells. (**C**) Single flat 'Subducted' cell external to early BLamD in atrophic area in perifovea. (**D**) Superimposed layers of 'Subducted' cells with evident melanosomes and LF/MLF granules at a GA border, defined by curved ELM (*green arrowheads*), in the fovea. ONL, outer nuclear layer.

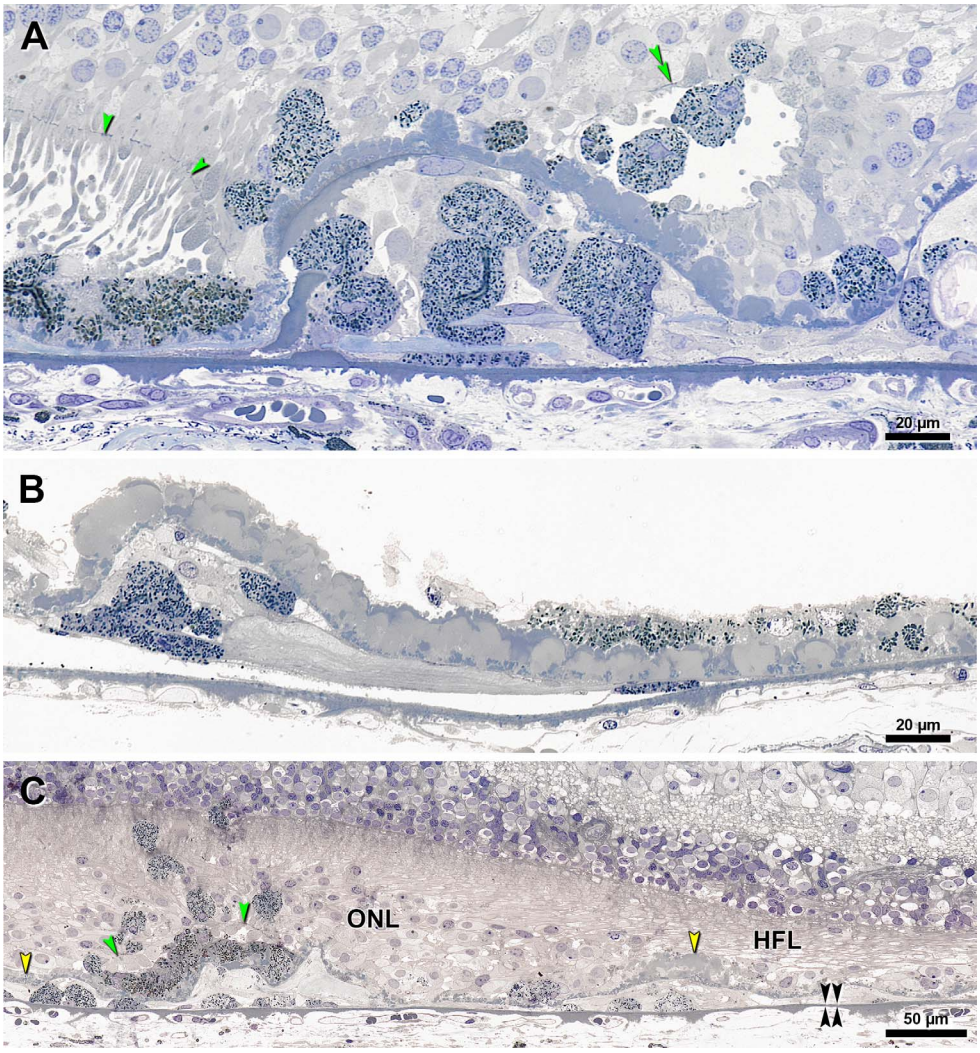

Figure 3. Transitions pertinent to 'Subducted' cells in eyes with GA. Submicrometer epoxy resin sections, toluidine blue stain. *Yellow arrowheads*, BLamD; *green arrowheads*, ELM; *double black arrowheads*, BrM. (**A**) At a GA border, in a Superior section, epithelial RPE is shown at the left, and persistent BLamD forms one complete corrugation[29] in the atrophic area. Atop the persistent BLamD are several 'Dissociated' RPE cells, which are spherical and are granule-rich, as is the epithelial RPE. These 'Dissociated' cells are quite similar to several 'Entubulated' cells in the lumen of outer retinal tubulation (*double green arrowheads*).[19] Strikingly, there is a break in the BLamD, with RPE breaking through to sub-RPE space. Within the central corrugation are eight cells, mostly spherical but one flattened, all with the same granule content of nearby RPE cells within the RPE layer. (**B**) Under a very thick layer of early and late BLamD are approximately six 'Subducted' cells ranging from spheroid to flattened, and all with dense granule content. On the *far right* is 'Dissociated' RPE, and shed granule aggregations within BLamD. One flat 'Subducted' cell underlies 'Very Nonuniform' RPE. Neurosensory retina is detached in this foveal region. (**C**) Sequence of 'Subducted' cells dedifferentiation in a parafoveal region. 'Subducted' cells on BrM are dome-shaped and granule-rich at the *left*. From *left to right*, into the atrophic area, cells progressively flatten and become granule-poor. From *left to right*, the grade of RPE cells internal to the BLamD changes from 'Intraretinal' to 'Dissociated' to 'Atrophy with BLamD.' HFL, Henle fiber layer.

three different eyes with GA. Granule-containing RPE was found breaking through a corrugation of persistent BLamD and entering the sub-RPE space (Fig. 3A), as if entering a building by climbing through a window. Spheroid and flattened granule-rich cells are external to thick late BLamD (Fig. 3B). A complete sequence of RPE transdifferentiation along BrM is apparent in a section passing through an island of RPE surviving between two GA lobules (Fig. 3C, green arrowheads indicate external limiting membrane [ELM] over RPE). In the sub-RPE space under the atrophic area on the left and under the surviving RPE are dome-shaped granule-rich cells. In the sub-RPE space to the right of the RPE island, extending throughout the main atrophic area, is a succession of progressively dedifferentiated, flattened, and degranulated cells.

The distribution of 'Subducted' cells in relation to the overlying RPE layer at the same locations is shown in Figure 4 and in Table 2 (pooled and per eye). 'Subducted' cells were more frequently encountered in GA eyes (13.1% of total locations) than in CNV eyes (4.8%). In GA eyes we found no relationship of 'Subducted' cells with subclasses of GA (central versus noncentral, unilobular versus multilobular,[7,22] width greater or less than the mean of the group). In CNV eyes, 29.2% of 'Subducted' cells were found underlying scars with 'Entombed' RPE (Table 2). If the 'Entombed' category is omitted, then the distribution of 'Subducted' cells by RPE grades in GA and CNV eyes can be compared directly. Comparing GA versus CNV, from greater to lesser frequency, we found 'Subducted' cells associated with 'Atrophy with BLamD' (32.2% vs. 37.0%), 'Dissociated' (22.0% vs. 21.7%),

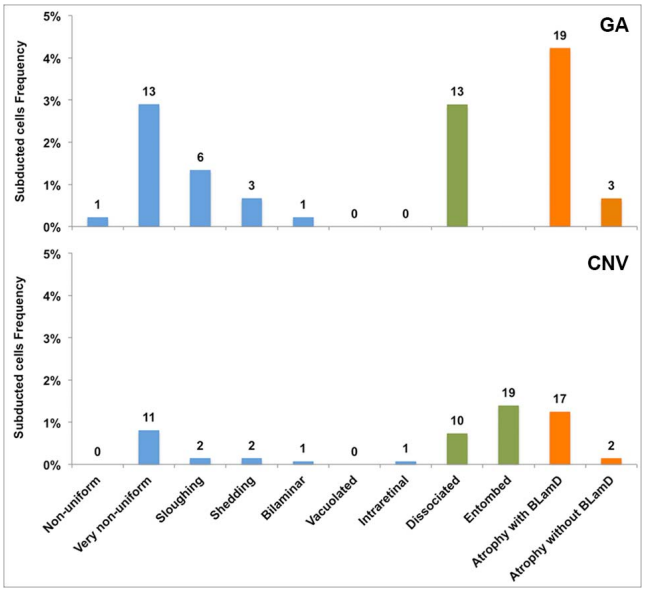

Figure 4. Association of *Subducted* cells with overlying RPE cells in eyes with GA and CNV. Superior and Central sections are combined. Epithelial, nonepithelial, and atrophic RPE morphologies, as defined in our companion article,[5] are indicated by *blue*, *green*, and *orange bars*, respectively. The percentages refer to total locations (see text). *Subducted* cells are more represented in GA eyes (59 locations, 13.1%) than CNV eyes (65 locations, 4.8%). They are associated with all grades, but especially in areas of advanced RPE change and RPE atrophy.

'Nonuniform' (22.0% vs. 23.9%), 'Sloughed' (10.2% vs. 4.3%), and the remaining grades. Thus, the distribution appears similar in GA and CNV, except for the association with 'Sloughed' cells, which are more frequently found in eyes with GA than in CNV.[5]

Exclusively found in eyes with CNV scars, 'Melanotic' cells were defined by a variable number of very dark, spherical melanosomes of different sizes (polydisperse) (Fig. 5). The largest melanosomes in 'Melanotic' cells (~3–5 μm) were larger than LF/MLF in these cells, and the edges of granules stained darker than the interiors (Figs. 5A, 5B). Spherical melanosomes in 'Melanotic' cells were easily distinguished from the small, monodisperse, and densely packed spherical melanosomes within choroidal melanocytes (Figs. 5B, 5D). Nuclei of 'Melanotic' cells and RPE cells were similar in size, shape, and chromatin patterns. 'Melanotic' cells were found in subretinal and sub-RPE spaces and could be inside scar or associated with scar in the other space, often arranged in one or multiple layers and surrounded by a hyaline envelope (Figs. 5A–C). Less frequently, 'Melanotic' cells were solitary. Like 'Entombed' RPE living within scars,[5] 'Melanotic' cells often assumed a rectangular solid shape, without detectable apical processes and containing little detectable LF/MLF except at specific transitions. Our impression was that 'Entombed' cells localized to both fibrovascular and fibrocellular scar, and in contrast, 'Melanotic' cells were present only in fibrocellular scar.

Evidence of cells in the same horizontal plane containing spindle-shaped and spherical melanosomes, sometimes within the same cells, were interpreted as evidence for transdifferentiation from 'Entombed' to 'Melanotic,' without precluding the possibility of 'Melanotic' arising independently from other sources. Figure 6 shows histology of a CNV eye with prominent black pigmentation in the fundus (see Appendix for link to this image). In the exemplar tableau of Figure 6, we show cells containing almost exclusively spindle-shaped melanosomes

Table 2. Associations of 'Subducted' RPE With Status of the RPE Cell Layer at the Same Location

	GA (Superior + Central)						CNV (Superior + Central)					
			% of 'Subducted' RPE at Each RPE Grade						% of 'Subducted' RPE at Each RPE Grade			
RPE Grade[5]	Total Locations	Locations With 'Subducted' RPE	Referenced to Total Locations	Referenced to Locations With 'Subducted' RPE	Referenced to Locations With 'Subducted' RPE	Referenced to 10 Grades Plus 'Entombed'	Total Locations	Locations With 'Subducted' RPE	Referenced to Total Locations	Referenced to Locations With 'Subducted' RPE	Referenced to 10 Grades	Referenced to 10 Grades Plus 'Entombed'
'Nonuniform'	80	1	0.2	1.7			36	0	0.0		0.0	0.0
'Very Nonuniform'	143	13	2.9	22.0			189	11	0.8		23.9	16.9
'Sloughed'	38	6	1.3	10.2			44	2	0.2		4.3	3.1
'Shedding'	39	3	0.7	5.1			25	2	0.2		4.3	3.1
'Bilaminar'	2	1	0.2	1.7			37	1	0.1		2.2	1.5
'Vacuolated'	1	0	0.0	0.0			5	0	0.0		0.0	0.0
'Intraretinal'	2	0	0.0	0.0			16	1	0.1		2.2	1.5
'Dissociated'	32	13	2.9	22.0			41	10	0.7		21.7	15.4
'Entombed'							302	19	1.4			29.2
'Atrophy with BLamD'	86	19	4.2	32.2			402	17	1.2		37.0	26.2
'Atrophy without BLamD'	26	3	0.7	5.1			266	2	0.1		4.3	3.1
Total	449	59	13.1	100.0			1363	65	4.8		100.0	100.0

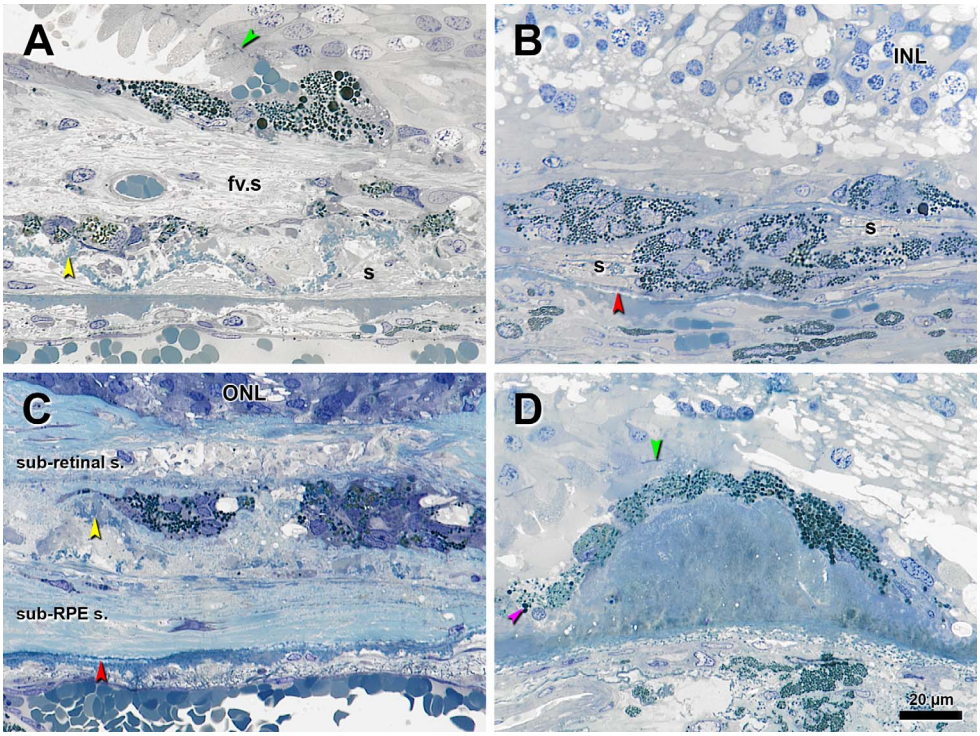

Figure 5. Melanotic cells in eyes with advanced AMD. Epoxy resin sections were stained with toluidine blue. *Yellow arrowheads*, BLamD; *red arrowhead*, calcification in BrM; *green arrowheads*, ELM. In (**B**) and (**D**), small spherical monodisperse melanosomes are evident in the choroid. (**A**) Pigmented cells containing dark, spherical, polydisperse melanosomes over a subretinal fibrovascular scar (fv.s) containing 'Entombed' RPE and persistent BLamD in a corrugated form. Fibrocellular scar in sub-RPE space(s). (**B**) Clusters of 'Melanotic' cells containing spherical polydisperse melanosomes inside and above a sub-RPE fibrous scar(s) without BLamD. These cells appear encapsulated by a *blue-staining*, likely collagenous material. (**C**) Group of 'Melanotic' cells, some with apparent cysts, surrounded by thick subretinal and sub-RPE fibrocellular scars divided by thin persistent BLamD. Some pigmented cells on the *right side* also contain few spindle-shaped melanosomes and gold-brown spherical granules, probably LF/MLF (**D**) In a singular finding, an RPE monolayer over a large hard druse in the peripapillary region continues as a monolayer of 'Melanotic' cells. Inside cells at the *left* are some spherical melanosomes (*pink arrowhead*).

(Fig. 6B), almost exclusively spherical melanosomes (Figs. 5C, 5D), and some with both melanosome types (Fig. 6E; also Figs. 5C, 5D). When in transition from 'Entombed' RPE, 'Melanotic' cells also could be interposed with intracellular (Fig. 5C) and extracellular (Fig. 6C) cystic spaces. Figure 5D shows another apparent transdifferentiation event not involving 'Entombed,' in which a druse is covered partially by 'Nonuniform' RPE and partially by 'Melanotic.'

'Melanotic' cells were much more abundant in the subretinal space (11.4% of total locations) than in the sub-RPE space (1.3%), and they were associated exclusively with advanced RPE grades within CNV eyes. Figure 7 illustrates the association of subretinal 'Melanotic' cells with each of the RPE morphologies in the overlying RPE layer. Of the observed subretinal 'Melanotic' cells, 40.0% were associated with 'Atrophy with BLamD,' 36.8% with 'Atrophy without BLamD,' 20.6% with 'Entombed,' and the remainder with other grades.

Discussion

Numerous RPE-derived cells survive in eyes at advanced AMD stages, confirming and quantifying a widespread impression of RPE hardiness. The newest morphologies herein defined are 'Subducted' cells containing RPE granules and dispersed along BrM, and 'Melanotic' cells that contribute black pigmentation to disciform scars. Previously we described another RPE-derived cell, 'Entubulated,' within the lumen of outer retinal tubulation.[19] These arise largely but not exclusively from 'Sloughed' RPE in preserved retina peripheral to the atrophic area[19] and account for the hyperreflective spots revealed by spectral-domain optical coherence tomography (SDOCT) in these formations. With 'Entubulated,' the descriptions of 'Subducted' and 'Melanotic' complete a graphical hypothesis for RPE pathways, including transdifferentiation, migration, and death in AMD (Fig. 1), begun in our companion article.[5] Together these two reports consolidate and codify voluminous histology literature (Table 3; table 5 of our companion paper[5]). They also amply demonstrate the diversity of RPE responses to stress, and by inference, the diversity of stresses eliciting these responses.

Subducted RPE

Our observations on 'Subducted' cells explain previous sightings of pigment-laden cells on BrM in AMD, including a cell with "processes, melanolipofuscin granules, [and a] nucleus similar to RPE"[23] and fully pigmented dome-shaped cells within a serous RPE detachment.[21] Panoramic views of histological sections that at best resemble low-magnification color electron microscopy disclosed transitional forms between pigmented cells in the RPE layer (usually atop BLamD), pigmented cells external to BLamD and on BrM, and progressive depigmentation and flattening. 'Subducted' cells are thus distinct from other cells described in relation to BrM and adjacent layers. These include (from inner to outer) Müller cells and microglia invading BLamD,[20,24,25] macrophages with intracellular lipid droplets[26] and giant multinucleate cells on BrM,[27–29] macrophages within BrM,[30] and phagocytes clearing choriocapillary endothelium external to BrM.[23,30]

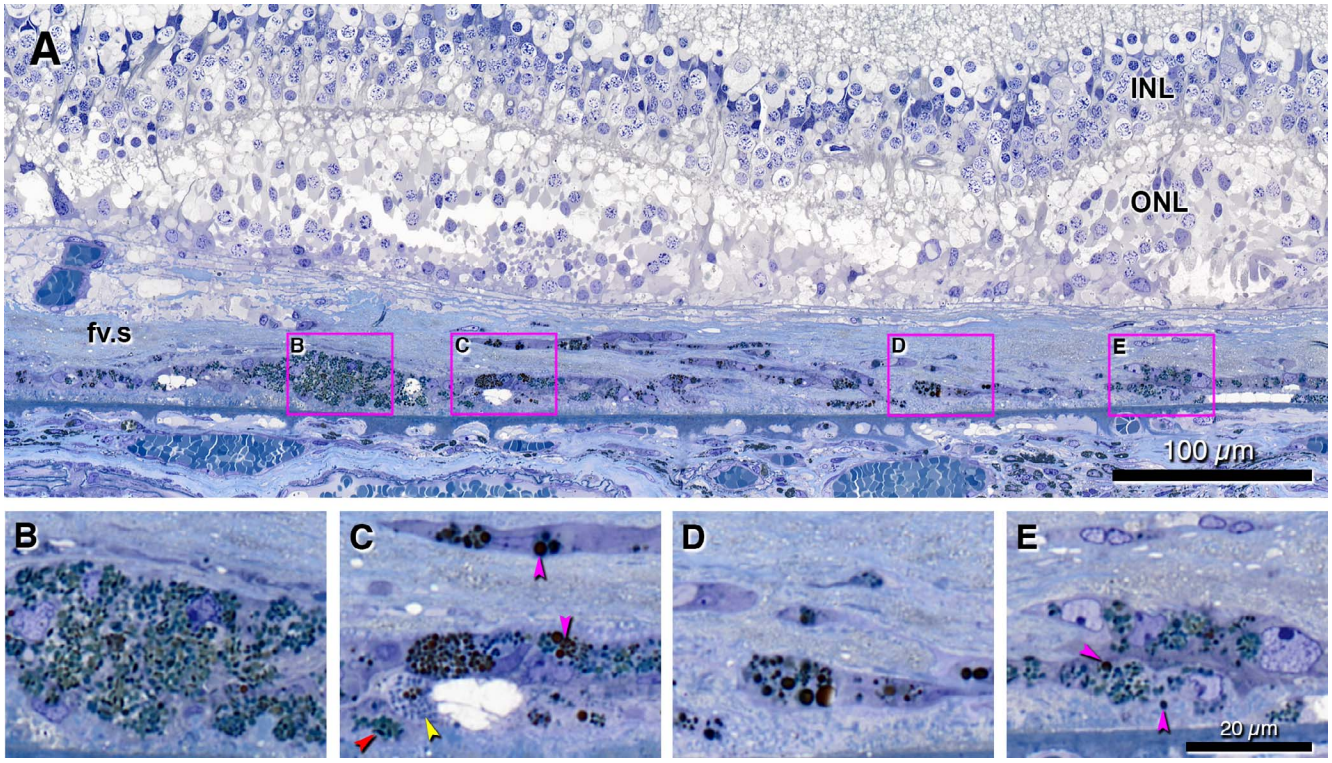

Figure 6. Retinal pigment epithelium transdifferentiation into 'Melanotic' cells. Submicrometer epoxy resin section, *toluidine blue stain*. The section corresponds to a heavily pigmented region on an ex vivo color fundus photograph (online eye #2009005R; link is in Appendix). *Scale bar* in (**E**) applies to (**B–E**). *Cyan arrowheads*, spindle-shaped melanosomes; *pink arrowheads*, spherical melanosomes**.** (**A**) Perifoveal subretinal fv.s containing transitions among different types of pigmented cells, organized in layers, some adherent to BLamD, and some interspersed with cystic spaces. Disorganized ONL with photoreceptor inner segments over the scar undulates, a pattern reminiscent of an outer retinal tubulation branch point.[19] *Boxes* indicate regions shown at higher magnification in (**B–E**). (**B**) Cluster of 'Melanotic' RPE cells with mostly spindle-shaped melanosomes and LF/MLF granules. (**C**) Cells containing three different types of granules: spindle-shaped melanosomes; small, uniform, spherical granules (probable LF/MLF; *yellow arrowheads*); and polydisperse dark spherical granules. A cystic space is present. (**D**) Cells with dark, polydisperse, and spherical granules inside fibrous tissue. (**E**) 'Melanotic' RPE containing both large and dark melanosomes and spindle-shaped melanosomes, close to early BLamD. A 'Subducted' cell is in sub-RPE space.

'Subducted' cells are common in GA and in locations with 'Atrophy with BLamD,' 'Dissociated' RPE, and 'Very Nonuniform' RPE (Fig. 4), prompting questions about their source. For three reasons we hypothesize that 'Subducted' cells originate from 'Dissociated' RPE present in the atrophic areas. First, 'Subducted' cells were rarely found in early AMD and normal eyes prepared in the same manner as these eyes (http://projectmacula.cis.uab.edu), although these impressions need verification via systematic review and our current nomenclature. Second, atrophic areas have many 'Dissociated' RPE,[5] which are not part of an intact epithelium and are therefore free to roam. Imaging suggests that pigmented entities in atrophic areas consistent with cells do roam, at least laterally.[31] Third, sources of cells in the relatively normal retina peripheral to atrophic areas are not obvious. The strong association of 'Subducted' with 'Very Nonuniform' is more likely due to the abundance of 'Very Nonuniform' in late AMD eyes,[5] rather than the subduction of 'Very Nonuniform' cells, in our view. The 'Shedding' RPE phenotype, which sheds granule aggregations

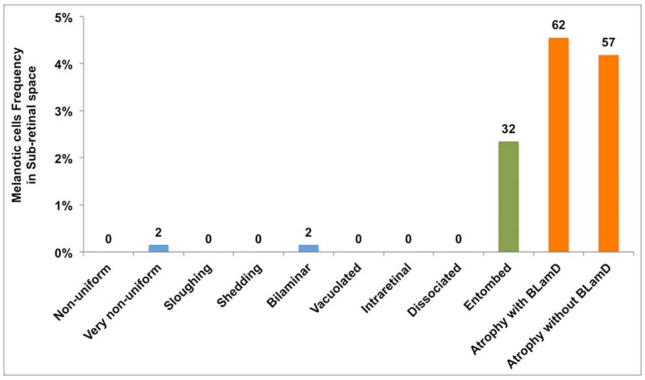

Figure 7. Melanotic cells distribution in subretinal space in CNV eyes. Epithelial, nonepithelial, and atrophic RPE morphologies are indicated by *blue*, *green*, and *orange bars*, respectively, as in Figure 4. The percentages refer to 1363 CNV locations analyzed for RPE and BLamD features.[5] 'Melanotic' cells were found only in CNV eyes, predominantly in subretinal space (11.4% of total locations) versus the sub-RPE space (1.3%). They were associated almost always with RPE atrophy and 'Entombed' RPE.

Table 3. Previous Literature on Histology and Imaging of RPE-Derived Cells

Morphology	Histology References	SDOCT References
'Subducted'	Fig. 2 (TEM)[23]; Fig. 2A[12]; Fig. 2G[21]	Figs. 4C, 7B[33]; Fig. 2E[34]
'Melanotic'	Fig. 4[29]	
'Entubulated'	Fig. 1[19]	

Published images were assigned to specific RPE-derived cells by authors ECZ and CAC using the definitions in the current article. TEM, transmission electron microscopy.

(possibly apoptotic bodies) into BLamD, is another possible source, but it does not seem to shed cells. One inference from this reasoning is that 'Subducted' cells originate from the atrophic area, break through BLamD by unknown mechanisms but likely involving protease activity, and move to relatively unaffected retina, facilitated in movements through the narrow sub-RPE space by a flat shape. Our forthcoming report on RPE morphologies relative to a GA border defined by ELM descent toward BrM[32,33] will further address this idea. Whether 'Subducted' cells are escaping from degeneration or emigrating toward relatively normal retina depends on the signals emitted from these two microenvironments. In this regard, 'Subducted' cells can be compared with 'Intraretinal' RPE, which apparently responds vigorously to stress signals in overlying neurosensory retina by migrating toward them.

Ideally, our snapshot histology can seed the process of identifying RPE morphologies by SDOCT, as demonstrated by direct clinicopathologic correlation for multiple morphologies, including granule aggregates (within BLamD) that are smaller than 'Subducted' cells.[5] However, the SDOCT correlate for 'Subducted' cells is currently unknown. We initially considered as a candidate the "highly reflecting, segmented plaques ... at the level of band 4 [RPE-BrM complex] ... that did not correlate with funduscopically visible drusen" (described in Refs. 33, 34; illustrated without comment in Ref. 35). Fleckenstein et al.[33] speculated that plaques corresponded to BrM densification (i.e., accumulation of electron-dense material[32,36] distinct from calcification), residual sub-RPE deposits, or regressing/calcifying drusen. Spectral-domain OCT plaques are horizontally elongated in shape, and located in the RPE-BrM complex, like 'Subducted' cells, yet plaque reflectivity seems too intense over too wide an area to be explained by cells, so we ultimately rejected this idea. Finding an imaging correlate for 'Subducted' may require a new technology, such as adaptive optics assisted near-infrared reflectance ophthalmoscopy.[31] Improved axial resolution for this technology, as well as for fundus autofluorescence, together with SDOCT, may allow 'Subducted' cells to be monitored in vivo. Importantly, longitudinal testing will allow determination of whether 'Subducted' cells are helpful or harmful.

Melanotic RPE

We saw embedded within fibrovascular scars plausible transitions of 'Entombed' RPE to cells with spherical black melanosomes (and nowhere else within early and late AMD eyes and normal eyes), supporting 'Melanotic' cells as RPE-derived. 'Melanotic' cells correspond to hyperpigmented features that are distinctively gray or black in ex vivo color photographs of donor eyes as they appear in vivo. Our results can be compared and contrasted with previous descriptions of RPE change in chorioretinal disease hinting at similar transformations.[37] In bone spicule degeneration of RP, cells with spherical melanosomes enter neurosensory retina and surround retinal blood vessels associated with a layered extracellular matrix resembling BrM.[37] In congenital retinal pigment epithelial hypertrophy, tall and focally multilayered RPE with large spherical melanosomes and no LF/MLF directly borders on normal RPE, in the RPE layer.[38,39] In congenital grouped pigmentation, corresponding to clinically apparent bear tracks, RPE cells of normal height contain numerous enlarged spindle-shaped melanosomes, distributed throughout the cell instead of just the apical aspect.[39] In AMD, mechanisms regulating conversion to 'Melanotic' are unknown but may include exposure to hemorrhage.[40] Functional consequences of 'Melanotic' cells are also unknown and may even be beneficial in slowing further CNV, as postulated for hyperpigmentation in pathologic myopia.[41]

Does RPE Undergo Transdifferentiation in AMD?

At three places in Figure 1, RPE cells attain different morphologies and different functional repertoires, including even migration ('Dissociated' to 'Subducted,' 'Entombed' to 'Melanotic,' and 'Sloughed' to 'Intraretinal'). It remains to be determined whether the cells in question are displaced and/or partially degenerated RPE that assumed different morphology but still retained their essential nature. Despite this uncertainty, it is tempting to revisit the hypothesis that in AMD, RPE undergoes transdifferentiation,[10,11] the process by which one differentiated cell type transforms to another cell type. Epithelium-to-mesenchymal transition is a well-studied exemplar transdifferentiation process in which a polarized epithelial cell on its basement membrane responds to its environment with loss of polarity, enhanced migratory capacity, invasiveness, elevated resistance to apoptosis, and increased production of extracellular matrix components. When EMT is complete, basement membrane degrades, and a mesenchymal cell migrates away from its layer of origin.[9,42,43] Key molecular events are de novo expression of α-smooth muscle actin, upregulation of the intermediate filament vimentin, and concomitant repression of cytokeratin. These events occur in RPE adopting contractile behavior in culture,[10] in RPE surgically excised from patients with proliferative vitreoretinopathy and neovascular AMD,[11,44] and in 'Sloughed' and 'Intraretinal' RPE from AMD eyes.[12] Immunoreactivity for α-smooth muscle actin[12] and the transmembrane protein CX3CR1[24] localizes to flat profiles on BrM consistent with 'Subducted' cells, yet not exhibiting RPE granules; these suggestive results should be revisited with higher-resolution labeling studies. Oncogenic EMT is further associated with defects in key tumor suppressors, including phosphatase and tensin homologue deleted on chromosome 10 (PTEN), a potent activator of the phosphoinositide 3-kinase signaling cascade.[45] In mice, this gene product strongly and preferentially localizes to basolateral RPE, relative to other retinal layers.[46] The PTEN-deficient RPE loses intercellular adhesions, upregulates motility genes, undergoes EMT, and migrates completely out of the eye.[46] These startling results suggest that under appropriate circumstances, RPE in vivo readily becomes migratory, due to an intrinsic motility that is normally countered within the epithelial layer by PTEN. We considered EMT because it is well characterized molecularly and because evidence currently exists for RPE, yet we emphasize that determining whether transdifferentiation is operative in AMD and how it takes place awaits new research.

Conclusions

'Melanotic' RPE in neovascular AMD importantly reminds us that the clinical appearance of both pigment variation and long-wavelength autofluorescence (attributed to melanin)[47] are both seen via a projection image in the en face view and are multifactorial in origin. Subcellular factors include the number, size, shape, and disposition of melanosomes within individual cells, and cellular-level factors include the shape and stacking of cells within the RPE layer. A similar argument was made for short-wavelength autofluorescence and LF/MLF.[7,48] All these phenomena invoke different molecular mechanisms in individual cells. Ophthalmologists have an unprecedented opportunity for molecular discovery if clinical observations can be informed by ultrastructural understanding of the organelle populations present at different stages of disease. The mechanisms regulating the size, shape, distribution, and imaging consequences of RPE melanosomes is thus an area

Investigative Ophthalmology & Visual Science

ripe for new investigation, and the benefit in accurately quantifying morphology will be large.

This report and its companion article[5] comprise an exhaustive and unbiased survey of RPE morphologies in AMD, and together should be viewed in light of limitations. These include small number of cells at some grades limiting the options for statistical analysis, nongeneralizability to the overall population due to the choice of eyes and sampling methods, lack of marker studies to supplement morphological definitions, and the requisite single-snapshot approach of histology.

Our survey, intended to provide a comprehensive context for clinical imaging, also helps identify major biologic effects, which will be priorities in future research. These effects are the numerous RPE cells surviving at end-stage disease ('Dissociated' and 'Entombed'), one main pathway of apparent cell death ('Shedding'), and multiple major pathways of apparent transdifferentiation ('Sloughed'/'Intraretinal,' 'Dissociated'/'Subducted,' 'Entombed'/'Melanotic'). Of the latter, 'Sloughed'/'Intraretinal' has known prognostic significance for progression of GA and CNV.[5] Our assessment demonstrates above all the amazing phenotypic diversity of RPE, a cell at the center of AMD. By highlighting transdifferentiation and its many implied molecular mechanisms, our data raise expectations for model systems used to test therapies for nonneovascular AMD, as these historically emphasize depigmentation and atrophy. Evidence for transdifferentiation also highlights the multiple microenvironments that replacement cells[49] will encounter in situ. Although RPE diversity imposes new challenges to preventing and treating AMD efficiently for the expanding aged population, as a scientific community we can meet these challenges, if we know about them. The visualization targets we provide for current clinical imaging with cellular-level resolution and new RPE-centered imaging technologies with molecular resolution[50] help meet these challenges.

NOTE: Cells resembling 'Subducted' exhibit immunoreactivity for macrophage marker CCR2 in human eyes with geographic atrophy.[51]

Acknowledgments

We thank the personnel of the Alabama Eye Bank (Doyce V. Williams, executive director, and Alan S. Blake, chief technical officer) for timely retrieval of donor eyes; donor families for their generosity; Nancy E. Medeiros, MD, for assistance in evaluating ophthalmic histories of eye donors; Kristen Hammack, BS, for ImageJ support; and Giovanni Staurenghi, MD, for facilitating the participation of author ECZ.

Supported by National Eye Institute Grants EY06109 (CAC), R01 EY015520 (RTS), and R01 EY 021470 (RTS), with institutional support from the EyeSight Foundation of Alabama and Research to Prevent Blindness, Inc. (CAC). Also supported by University of Milan (ECZ) and DFG (German Research Foundation) Grants AC265/1-1 and AC265/2-1 (TA). Acquisition of donor eyes was supported by International Retinal Research Foundation, National Eye Institute P30 EY003039, and the Arnold and Mabel Beckman Initiative for Macular Research. Creation of Project MACULA was additionally supported from the Edward N. and Della L. Thome Memorial Foundation.

Disclosure: **E.C. Zanzottera**, None; **J.D. Messinger**, None; **T. Ach**, None; **R.T. Smith**, None; **C.A. Curcio**, None

References

1. Fritsche LG, Fariss RN, Stambolian D, Abecasis G, Curcio CA, Swaroop A. Age-related macular degeneration: genetics and biology coming together. *Annu Rev Genomics Hum Genet*. 2014;15:151–171.
2. Shi G, Maminishkis A, Banzon T, et al. Control of chemokine gradients by the retinal pigment epithelium. *Invest Ophthalmol Vis Sci*. 2008;49:4620–4630.
3. Curcio CA. Complementing apolipoprotein secretion by retinal pigment epithelium. *Proc Natl Acad Sci U S A*. 2011; 108:18569–18570.
4. Booij JC, ten Brink JB, Swagemakers SM, et al. A new strategy to identify and annotate human RPE-specific gene expression. *PLoS One*. 2010;5:e9341.
5. Zanzottera EC, Messinger JD, Ach T, Smith RT, Freund KB, Curcio CA. The Project MACULA retinal pigment epithelium grading system for histology and optical coherence tomography in age-related macular degeneration. *Invest Ophthalmol Vis Sci*. 2015;56:3253–3268.
6. Vogt SD, Curcio CA, Wang L, et al. Retinal pigment epithelial expression of complement regulator CD46 is altered early in the course of geographic atrophy. *Exp Eye Res*. 2011;93:413–423.
7. Rudolf M, Vogt SD, Curcio CA, et al. Histologic basis of variations in retinal pigment epithelium autofluorescence in eyes with geographic atrophy. *Ophthalmology*. 2013;120:821–828.
8. Shen CN, Burke ZD, Tosh D. Transdifferentiation, metaplasia and tissue regeneration. *Organogenesis*. 2004;1:36–44.
9. Puisieux A, Brabletz T, Caramel J. Oncogenic roles of EMT-inducing transcription factors. *Nat Cell Biol*. 2014;16:488–494.
10. Grisanti S, Guidry C. Transdifferentiation of retinal pigment epithelial cells from epithelial to mesenchymal phenotype. *Invest Ophthalmol Vis Sci*. 1995;36:391–405.
11. Lopez PF, Sippy BD, Lambert HM, Thach AB, Hinton DR. Transdifferentiated retinal pigment epithelial cells are immunoreactive for vascular endothelial growth factor in surgically excised age-related macular degeneration-related choroidal neovascular membranes. *Invest Ophthalmol Vis Sci*. 1996;37: 855–868.
12. Guidry C, Medeiros NE, Curcio CA. Phenotypic variation of retinal pigment epithelium in age-related macular degeneration. *Invest Ophthalmol Vis Sci*. 2002;43:267–273.
13. Curcio CA, Sloan KR, Kalina RE, Hendrickson AE. Human photoreceptor topography. *J Comp Neurol*. 1990;292:497–523.
14. Schraermeyer U, Heimann K. Current understanding on the role of retinal pigment epithelium and its pigmentation. *Pigment Cell Res*. 1999;12:219–236.
15. Dell'Angelica EC, Mullins C, Caplan S, Bonifacino JS. Lysosome-related organelles. *FASEB J*. 2000;14:1265–1278.
16. Weiter JJ, Delori FC, Wing GL, Fitch KA. Retinal pigment epithelial lipofuscin and melanin and choroidal melanin in human eyes. *Invest Ophthalmol Vis Sci*. 1986;27:145–152.
17. Feeney-Burns L, Hilderbrand E, Eldridge S. Aging human RPE: morphometric analysis of macular, equatorial, and peripheral cells. *Invest Ophthalmol Vis Sci*. 1984;25:195–200.
18. Green WR, Enger C. Age-related macular degeneration histopathologic studies: the 1992 Lorenz E. Zimmerman Lecture. *Ophthalmology*. 1993;100:1519–1535.
19. Schaal KB, Freund KB, Litts KM, Zhang Y, Messinger JD, Curcio CA. Outer retinal tubulation in age-related macular degeneration: optical coherence tomographic findings correspond with histology [published online ahead of print January 29, 2015]. *Retina*. PMID 25635579.
20. Gupta N, Brown KE, Milam AH. Activated microglia in human retinitis pigmentosa, late-onset retinal degeneration, and age-related macular degeneration. *Exp Eye Res*. 2003;76:463–471.
21. Curcio CA. Imaging maculopathy in the post-mortem human retina. *Vision Res*. 2005;45:3496–3503.
22. Xu L, Blonska AM, Pumariega N, et al. Reticular macular disease is associated with multilobular geographic atrophy in

age- related macular degeneration. *Retina*. 2013;33:1850–1862.

23. Killingsworth MC, Sarks JP, Sarks SH. Macrophages related to Bruch's membrane in age-related macular degeneration. *Eye*. 1990;4:613–621.
24. Combadière C, Feumi C, Raoul W, et al. CX3CR1-dependent subretinal microglia cell accumulation is associated with cardinal features of age-related macular degeneration. *J Clin Invest*. 2007;117:2920–2928.
25. Ma W, Coon S, Zhao L, Fariss RN, Wong WT. A2E accumulation influences retinal microglial activation and complement regulation. *Neurobiol Aging*. 2013;34:943–960.
26. Curcio CA, Medeiros NE, Millican CL. Photoreceptor loss in age-related macular degeneration. *Invest Ophthalmol Vis Sci*. 1996;37:1236–1249.
27. Penfold PL, Killingsworth MC, Sarks SH. Senile macular degeneration: the involvement of immunocompetent cells. *Graefes Arch Clin Exp Ophthalmol*. 1985;223:69–76.
28. Penfold PL, Killingsworth MC, Sarks SH. Senile macular degeneration. The involvement of giant cells in atrophy of the retinal pigment epithelium. *Invest Ophthalmol Vis Sci*. 1986;27:364–371.
29. Ooto S, Vongkulsiri S, Sato T, Suzuki M, Curcio CA, Spaide RF. Outer retinal corrugations in age-related macular degeneration. *JAMA Ophthalmol*. 2014;132:806–813.
30. Sarks JP, Sarks SH, Killingsworth MC. Morphology of early choroidal neovascularization in age-related macular degeneration: correlation with activity. *Eye*. 1997;11:515–522.
31. Gocho K, Sarda V, Falah S, et al. Adaptive optics imaging of geographic atrophy. *Invest Ophthalmol Vis Sci*. 2013;54:3673–3680.
32. Sarks JP, Sarks SH, Killingsworth MC. Evolution of geographic atrophy of the retinal pigment epithelium. *Eye*. 1988;2:552–577.
33. Fleckenstein M, Charbel Issa P, Helb HM, et al. High-resolution spectral domain-OCT imaging in geographic atrophy associated with age-related macular degeneration. *Invest Ophthalmol Vis Sci*. 2008;49:4137–4144.
34. Moussa K, Lee JY, Stinnett SS, Jaffe GJ. Spectral domain optical coherence tomography-determined morphologic predictors of age-related macular degeneration-associated geographic atrophy progression. *Retina*. 2013;33:1590–1599.
35. Schmitz-Valckenberg S, Fleckenstein M, Helb HM, Charbel Issa P, Scholl HP, Holz FG. In vivo imaging of foveal sparing in geographic atrophy secondary to age-related macular degeneration. *Invest Ophthalmol Vis Sci*. 2009;50:3915–3921.
36. Green WR, Key SN III. Senile macular degeneration: a histopathologic study. *Trans Am Ophthalmol Soc*. 1977;75:180–254.
37. Li Z-Y, Possin DE, Milam AH. Histopathology of bone spicule pigmentation in retinitis pigmentosa. *Ophthalmology*. 1995;102:805–816.
38. Lloyd WC III, Eagle RC Jr, Shields JA, Kwa DM, Arbizo VV. Congenital hypertrophy of the retinal pigment epithelium. Electron microscopic and morphometric observations. *Ophthalmology*. 1990;97:1052–1060.
39. Regillo CD, Eagle RC Jr, Shields JA, Shields CL, Arbizo VV. Histopathologic findings in congenital grouped pigmentation of the retina. *Ophthalmology*. 1993;100:400–405.
40. Green WR, McDonnell PJ, Yeo JH. Pathologic features of senile macular degeneration. *Ophthalmology*. 1985;92:615–627.
41. Parodi MB, Da Pozzo S, Ravalico G. Retinal pigment epithelium changes after photodynamic therapy for choroidal neovascularization in pathological myopia. *Acta Ophthalmol Scand*. 2007;85:50–54.
42. Kalluri R, Weinberg RA. The basics of epithelial-mesenchymal transition. *J Clin Invest*. 2009;119:1420–1428.
43. Lamouille S, Xu J, Derynck R. Molecular mechanisms of epithelial-mesenchymal transition. *Nat Rev Mol Cell Biol*. 2014;15:178–196.
44. Feist RM Jr, King JL, Morris R, Witherspoon CD, Guidry C. Myofibroblast and extracellular matrix origins in proliferative vitreoretinopathy. *Graefes Arch Clin Exp Ophthalmol*. 2014;252:347–357.
45. Song MS, Salmena L, Pandolfi PP. The functions and regulation of the PTEN tumour suppressor. *Nat Rev Mol Cell Biol*. 2012;13:283–296.
46. Kim JW, Kang KH, Burrola P, Mak TW, Lemke G. Retinal degeneration triggered by inactivation of PTEN in the retinal pigment epithelium. *Genes Dev*. 2008;22:3147–3157.
47. Keilhauer CN, Delori FC. Near-infrared autofluorescence imaging of the fundus: visualization of ocular melanin. *Invest Ophthalmol Vis Sci*. 2006;47:3556–3564.
48. Ach T, Tolstik E, Messinger JD, Zarubina AV, Heintzmann R, Curcio CA. Lipofuscin redistribution and loss accompanied by cytoskeletal stress in retinal pigment epithelium of eyes with age-related macular degeneration. *Invest Ophthalmol Vis Sci*. 2015;56:3242–3252.
49. Schwartz SD, Regillo CD, Lam BL, et al. Human embryonic stem cell-derived retinal pigment epithelium in patients with age-related macular degeneration and Stargardt's macular dystrophy: follow-up of two open-label phase 1/2 studies. *Lancet*. 2015;385:509–516.
50. Smith RT, Post R, Johri A, et al. Simultaneous decomposition of multiple hyperspectral datasets: fluorophore signal recovery in the retinal pigment epithelium (RPE). *Biomed Opt Express*. 2014;5:4171–4185.
51. Sennlaub F, Auvynet C, Calippe B, et al. CCR2(+) monocytes infiltrate atrophic lesions in age-related macular disease and mediate photoreceptor degeneration in experimental subretinal inflammation in Cx3cr1 deficient mice. *EMBO Mol Med*. 2013;5:1775–1793.

Appendix

Key to Figures at http://projectmacula.cis.uab.edu

Figure 2. Subducted RPE.
- (A) Section 2002002L-88F-4025, Eccentricity −540 (parafovea)
- (B) Section 2011017R-83F-4000, Eccentricity 0 (fovea)
- (C) Section 2011013R-95M-3975, Eccentricity −2100 (perifovea)
- (D) Section 2009001L-87M-4100, Eccentricity 400 (fovea)

Figure 3. Subduction of RPE cells under the RPE layer.
- (A) Section 2009001L-87M-2250 Eccentricity 1000 (parafovea) Not online
- (B) Section 2003029L-85F-3900, Eccentricity −110 (fovea)
- (C) Section 2008007L-76F-0 Eccentricity −550 (parafovea) Not online

Figure 5. Melanotic cells.
- (A) Section 0099013L-80F-4050 ecc. 200 (fovea)
- (B) Section 0096047L-94F-4000 ecc. 1600 (perifovea)
- (C) Section 2000056L-88F-2000 ecc. 0 (perifovea)
- (D) Section 0096047L-94F-4000 ecc. −3100 (near periphery)

Figure 6. RPE transdifferentiation into melanotic cells. Section 2009005R-83M-4050 ecc.1765 (perifovea)

Investigative Ophthalmology & Visual Science